Available online at www.sciencedirect.com
SCIENCE DIRECT®
Journal of Solid State Chemistry 177 (2004) 1592–1597
JOURNAL OF SOLID STATE CHEMISTRY
http://elsevier.com/locate/jssc

Synthesis and structural studies of $Sr_2Co_{2-x}Al_xO_5$, $0.3 \leqslant x \leqslant 0.5$

F. Lindberg,[a,*] G. Svensson,[a] S.Ya. Istomin,[b] S.V. Aleshinskaya,[c] and E.V. Antipov[b]

[a] *Department of Structural Chemistry, Stockholm University, Stockholm SE-10691, Sweden*
[b] *Department of Chemistry, Moscow State University, Moscow 119992, Russia*
[c] *Department of Materials Chemistry, Moscow State University, Moscow 119992, Russia*

Received 25 June 2003; received in revised form 28 November 2003; accepted 14 December 2003

Abstract

$Sr_2Co_{2-x}Al_xO_5$, $0.3 \leqslant x \leqslant 0.5$, with a perovskite related structure has been synthesized. The XRD powder patterns showed reflections from the basic cubic perovskite structure along with some additional weak superstructure reflections. Electron diffraction (ED) and high-resolution transmission electron microscopy (HRTEM) studies show that crystallites of $Sr_2Co_{2-x}Al_xO_5$ consist of small intergrown differently oriented domains, about 40 Å in diameter, with brownmillerite structure.

Keywords: Complex cobalt oxides; Brownmillerite structure; Electron diffraction; HRTEM

1. Introduction

The brownmillerite type structure $A_2B_2O_5$ represents one of the most common types of ordering of oxygen vacancies in oxygen-deficient perovskites. The structure can be described as consisting of alternating layers of BO_6 octahedra and BO_4 tetrahedra, see Fig. 1. It is found among complex first-row transition metal oxides, of manganese (Sr_2GaMnO_5 [1,2], Ca_2GaMnO_5 [3]), iron ($Ca_2(FeAl)O_5$ [4,5], Ca_2GaFeO_5 [6], $Sr_2Fe_2O_5$ [7], $Ca_2Fe_2O_5$ [8]), cobalt ($La_2Co_2O_5$ [9], $Sr_2Co_2O_5$ [10], $Ca_2(Co,Al)O_5$ [11]) and copper ($LaSrCuGaO_5$ [12]). Depending on the nature of the B cation and the synthesis conditions used, compounds with brownmillerite structure generally crystallize with one of three space group symmetries: *Ibm2*, *Pcmn* and *Icmm*. The first two space groups represent ordered variants of the structure, which differ from each other by the relative orientation of the chains of tetrahedra in different layers. The structure in space group *Icmm* comprises incomplete ordering of the chains within the tetrahedral layers. One example of an intermediate between the ordered structure in space groups *Ibm2*, *Pcmn* and the disordered in space group *Icmm* is the recently reported compound $Ca_2(Co,Al)O_5$ [11], with a modulated brownmillerite type structure due to long-range ordering of the chains of tetrahedra.

Recently we have successfully stabilized the brownmillerite structure for $Sr_2Co_2O_5$ by replacing Co^{3+} by Ga^{3+}: $Sr_2Co_{2-x}Ga_xO_5$, $0.3 \leqslant x \leqslant 0.8$ [13]. Here we present the preparation and electron microscopy studies of new complex cobalt oxides with composition $Sr_2Co_{2-x}Al_xO_5$.

2. Experimental

Samples of $Sr_2Co_{2-x}Al_xO_5$, $0.2 \leqslant x \leqslant 0.7$, $\Delta x = 0.1$, were synthesized from stoichiometric mixtures of $SrCO_3$, Al_2O_3 and Co_3O_4 (all reagents of analytical grade). The mixtures were first annealed in air at 1100°C for 24 h followed by regrinding and then reheating at 1250°C for 9 days, with 2 intermediate regrindings. The furnace was then shut off and the samples cooled to room temperature. Phase analysis of the products was made by means of their X-ray powder diffraction photographs, recorded with a Guinier–Hägg camera with focusing geometry, using Cu$K\alpha$1 radiation and Ge as an internal standard.

X-ray powder diffraction (XRPD) data were collected from the samples on a STOE STADI-P diffractometer in symmetric transmission mode and equipped with a linear position sensitive detector (mini-PSD) covering 4.6° in 2Θ.

*Corresponding author. Fax: +46-8-163118.
E-mail address: fredrik@struc.su.se (F. Lindberg).

0022-4596/$ - see front matter © 2004 Elsevier Inc. All rights reserved.
doi:10.1016/j.jssc.2003.12.012

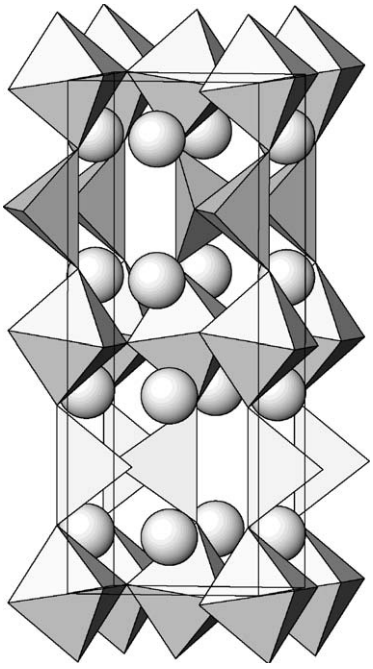

Fig. 1. The brownmillerite structure.

For transmission electron microscopy studies, small amounts of the samples were crushed in *n*-butanol. A drop of this dispersion was put on a holey carbon film supported by a copper grid. Electron diffraction (ED) studies and microanalysis were made in an JEOL JEM2000 FX instrument operated at 200 kV, equipped with a LINK AN10000 energy-dispersive X-ray microanalysis (EDX) system. High-resolution transmission electron microscopy (HRTEM) studies were made in a JEOL JEM3010 UHR microscope operated at 300 kV. Simulated HRTEM images were calculated with the program suite NCEMSS [14].

Iodometric titration was used to determine the oxygen content in the as-prepared samples with $0.3 \leqslant x \leqslant 0.8$. About 50 mg of the sample under investigation was placed in a flask containing 20 mL of a 20% water solution of KI. Then several drops of concentrated HCl were added to the solution. The flask was stored in a dark place until the entire sample had dissolved. The released elementary iodine was titrated with a standard $Na_2S_2O_3$ solution with starch added as an indicator.

3. Results and discussion

Single-phase samples of $Sr_2Co_{2-x}Al_xO_5$ have been prepared in the compositional range $0.3 \leqslant x \leqslant 0.5$ at 1250°C. At lower annealing temperatures multiphase samples were obtained. Examination of the XRPD patterns of $Sr_2Co_{2-x}Al_xO_5$ revealed the presence of a perovskite subcell ($a_{per} \approx 3.88$ Å, per = perovskite subcell), and supercell reflections with maximum intensity of 5%, see Fig. 2. Although there was no observable splitting of the perovskite subcell reflections, we could not accurately index the superstructure reflections with a double cubic perovskite unit cell ($a \approx 2 \times a_{per}$). However, they can be rather satisfactorily indexed with a tetragonal unit cell: $a \approx a_{per}$, $c \approx 2 \times a_{per}$, yielding the following refined unit cell parameters for the $x = 0.3$ composition: $a = 3.898(2)$, $c = 7.799(1)$. For $x = 0.4$, $a = 3.8963(7)$, $c = 7.790(3)$; and for $x = 0.5$, $a = 3.885(2)$, $c = 7.786(3)$ Å. Careful examination of the XRPD pattern of $Sr_2Co_{1.5}Al_{0.5}O_5$ (Fig. 2) revealed that some reflections, especially those indicating the supercell (odd values of *l*), have much larger FWHM values than the majority of perovskite substructure reflections. This does not involve the 1 1 2 reflection (the indexing refers to the tetragonal unit cell, $1\,1\,2 = 1\,1\,1_{per}$). This reflection is much wider than 103 of the superstructure. Such broadening of the 1 1 2 reflection, together with its strong asymmetry, indicates that the real symmetry of the structure is lower than tetragonal.

One can assume that peculiarities of the reflection profiles for $Sr_2Co_{2-x}Al_xO_5$ might be caused by disorder of the oxygen vacancies in the structure, as an effect of the high synthesis temperature used. However, reannealing of the prepared compounds at lower temperatures down to 1050°C did not influence the variation of FWHM with 2Θ. Decreasing the temperature to 950°C led to decomposition of $Sr_2Co_{2-x}Al_xO_5$. This is not surprising, since both $Sr_2Co_2O_5$ [15] and $Sr_2Co_{2-x}Ga_xO_5$ [13] have been found to be unstable under such conditions. The oxygen content of $Sr_2Co_{2-x}Al_xO_5$ remained stoichiometric within 2 e.s.d. for all compositions, as revealed by iodometric titration. EDS analysis revealed cation compositions close to nominal: $Sr_{2.00}Co_{1.72}Al_{0.27}O_x$, $Sr_{2.00}Co_{1.62}Al_{0.33}O_x$ and $Sr_{2.00}Co_{1.38}Al_{0.42}O_x$ for the samples with nominal Al compositions 0.3, 0.4 and 0.5, respectively.

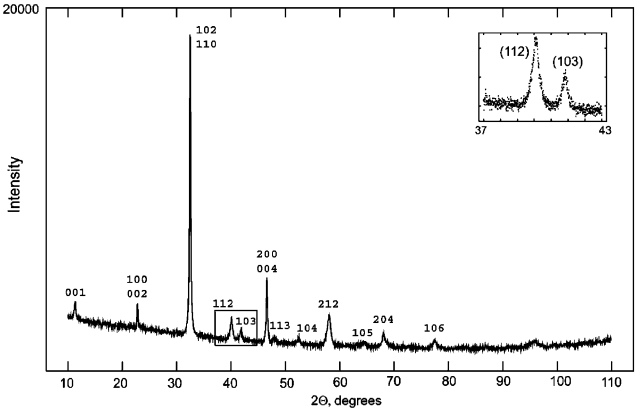

Fig. 2. X-ray diffraction pattern of $Sr_2Co_{1.5}Al_{0.5}O_5$ ($a = 3.885(2)$, $c = 7.786(3)$ Å). Superstructure reflections in relation to cubic perovskite are those with odd values of *l*. The perovskite subcell reflections 1 1 2 (or $1\,1\,1_{per}$) and neighboring superstructure reflection 1 0 3 are framed.

3.1. Electron diffraction and HRTEM studies

Investigation of ED patterns and HRTEM images of $Sr_2Co_{2-x}Al_xO_5$ ($0.3 \leqslant x \leqslant 0.5$) shows features that are not explained by the XRD study. ED and HRTEM micrographs reveal domains of ordered regions of the brownmillerite-type structure, altering with layers of octahedra and tetrahedra (Fig. 1). All the crystallites studied yielded ED patterns with superstructure reflections in addition to the perovskite subcell spots. Three such zone-axis patterns from one crystallite, recorded during a tilting experiment, are shown in Fig. 3a–c. The

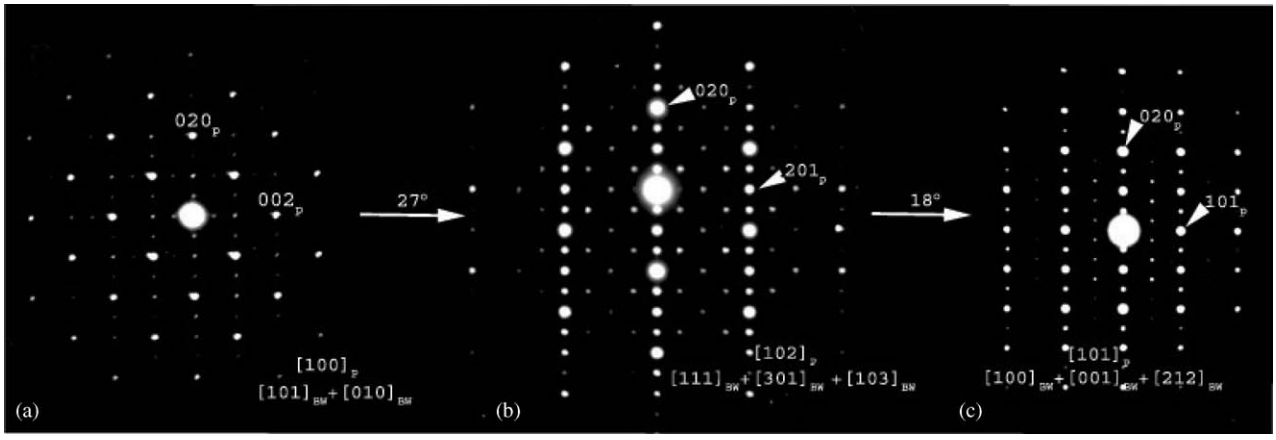

Fig. 3. (a) ED pattern recorded along the $\langle 001 \rangle_{per}$ perovskite subcell axis. Supercell reflections can be indexed with a $[101]_{BM}$ zone-axis pattern. (b) Tilting 27° around the $\langle 010 \rangle_{per}$ axis gives the $\langle 102 \rangle_{per}$ zone-axis pattern, with the reflections from the brownmillerite zone-axis patterns $[111]_{BM}$ and $[301]_{BM}$ (=[103]) superposed, which result from tilting 27° out of $[010]_{BM}$ and $[101]_{BM}$, respectively. (c) Further tilting, 18° from (b), gives sub-zone-axis pattern $\langle 101 \rangle_{per}$ along with reflections from $[100]_{BM}$, $[001]_{BM}$ and $[212]_{BM}$.

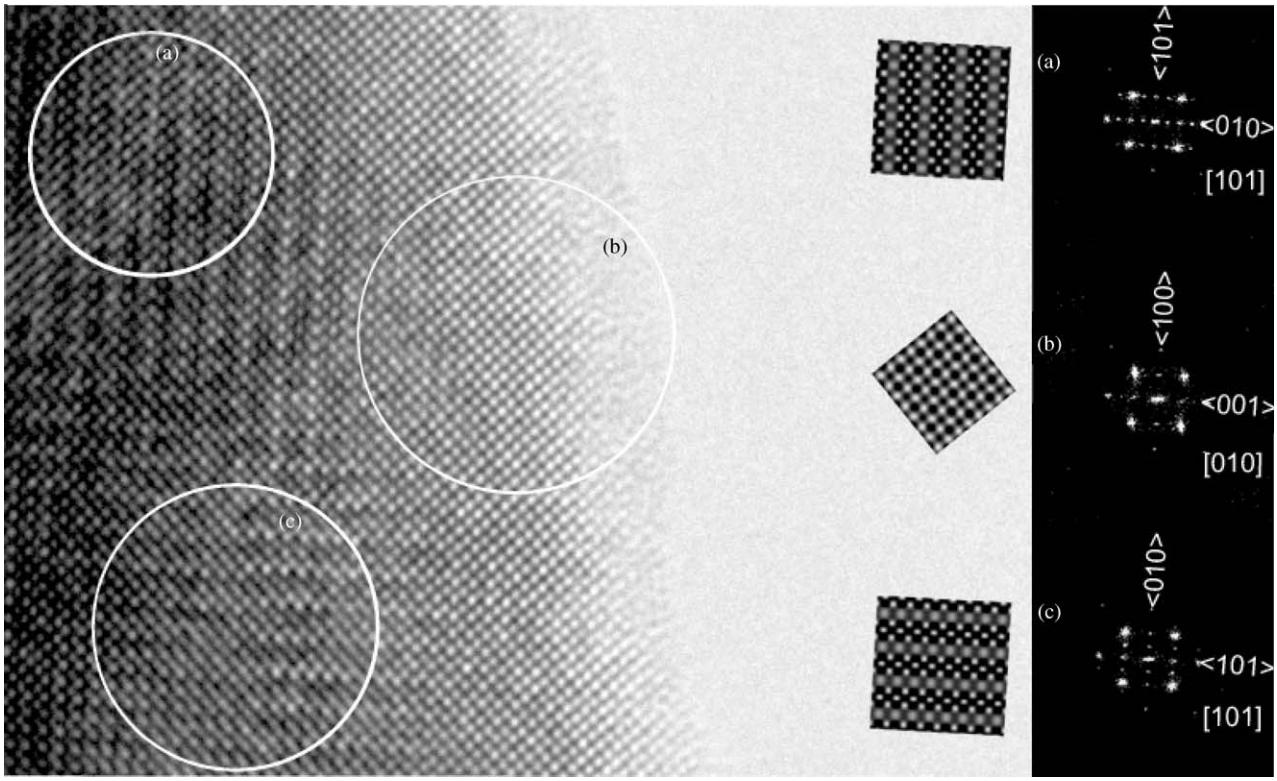

Fig. 4. High-resolution electron micrographs corresponding to the electron diffraction pattern shown in Fig. 3a. Fast Fourier transforms of the circled areas and calculated images of zone-axis $[101]_{BM}$ (a and c, at 90° to each other) and $[010]_{BM}$ (b) are shown in the right part of the figure. The simulated HRTEM images were calculated using the atomic coordinates for $Sr_2Co_{1.3}Ga_{0.7}O_5$ (space-group *Icmm*) [13] and with $C_s = 0.60$ mm, $C_c = 70$ Å, objective aperture 0.70 $Å^{-1}$, defocus = −290 Å and crystal thickness 10 Å (b) and 50 Å (a and c).

supercell reflections could not be accounted for by the tetragonal unit cell ($a = a_{per}$, $c = 2a_{per}$) found by XRD, see above. All the superstructure reflections could be successfully indexed with an orthorhombic unit cell: $a \approx c \approx \sqrt{2} \times a_{per}$ and $b \approx 4 \times a_{per}$, suggesting the presence of ordering of the brownmillerite type at the microstructure level. As can be seen in Fig. 3a, the ED pattern clearly reveals the perovskite subcell, because it can be indexed with the $\langle 001 \rangle_{per}$ zone-axis. The supercell reflections can be explained as coming from differently oriented domains of brownmillerite type structure along the $[101]_{BM}$ (BM = brownmillerite) zone axis at right angles to each other. The corresponding HRTEM image supports this explanation, see Fig. 4. It is clearly seen that the crystallite consists of small domains marked *a* and *c*, oriented at 90° to each other. The fast Fourier transform (FFT), shown in the right part of Fig. 4, further supports the assumption of differently oriented $[101]_{BM}$ domains. This image also reveals another type of domain within the thinnest part of the crystal, sharing the same perovskite sub-axis, marked as *b* and oriented along the $[010]_{BM}$ zone axis, as can be seen in the

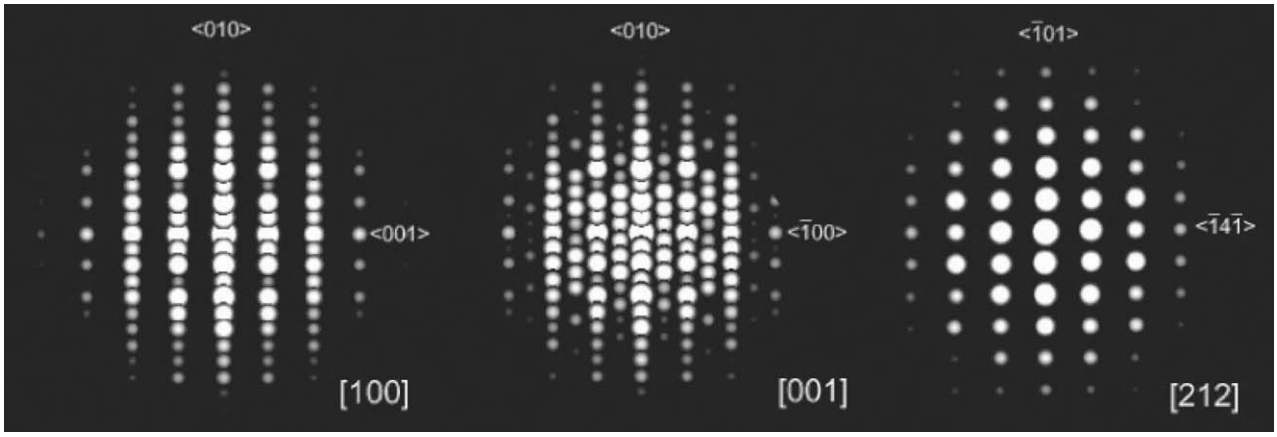

Fig. 5. Simulated ED patterns [100], [001] and [212], which together form the experimental composite zone-axis pattern seen in Fig. 3c.

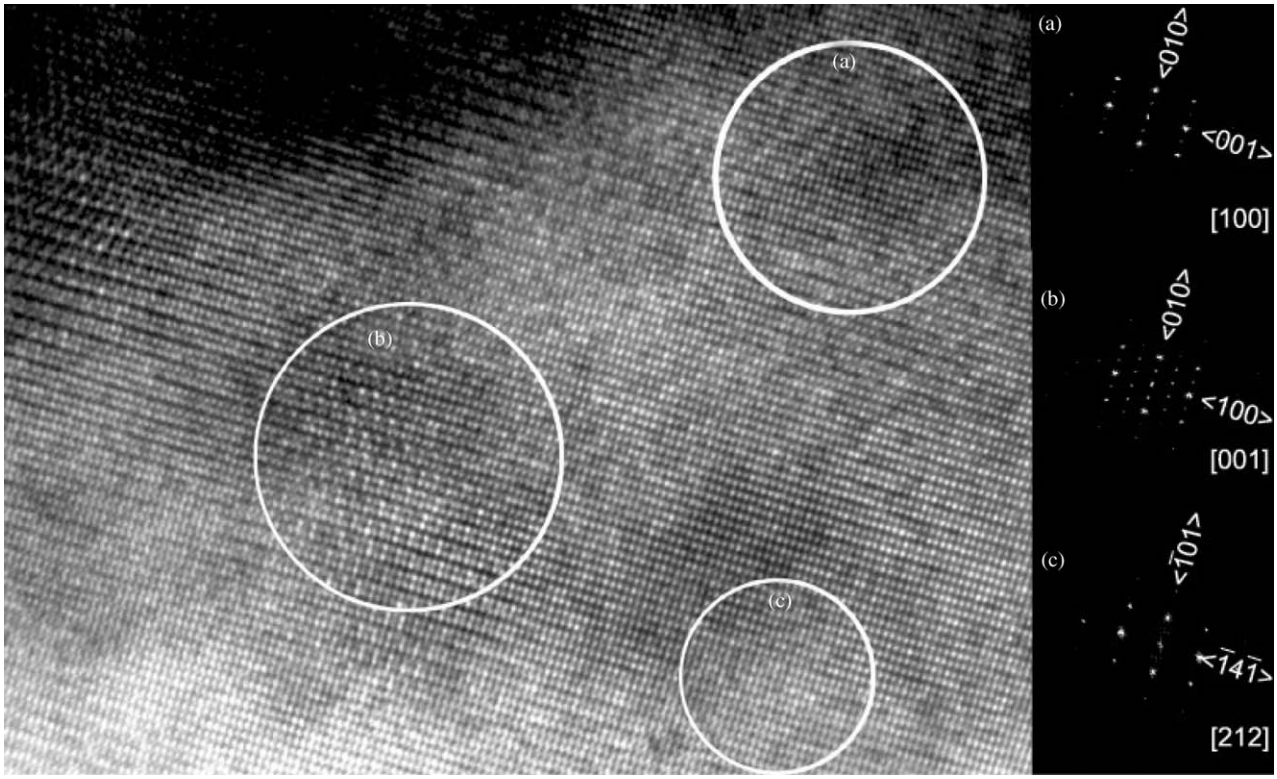

Fig. 6. High-resolution electron micrographs that reveal the mixing of the tree domains $[001]_{BM}$ (a), $[100]_{BM}$ (b), and $[212]_{BM}$ (c) suggested by the tilting experiment, all with common perovskite sub-cell zone-axis $\langle 101 \rangle_{per}$. FFTs of the circled areas are shown in the right part of the figure.

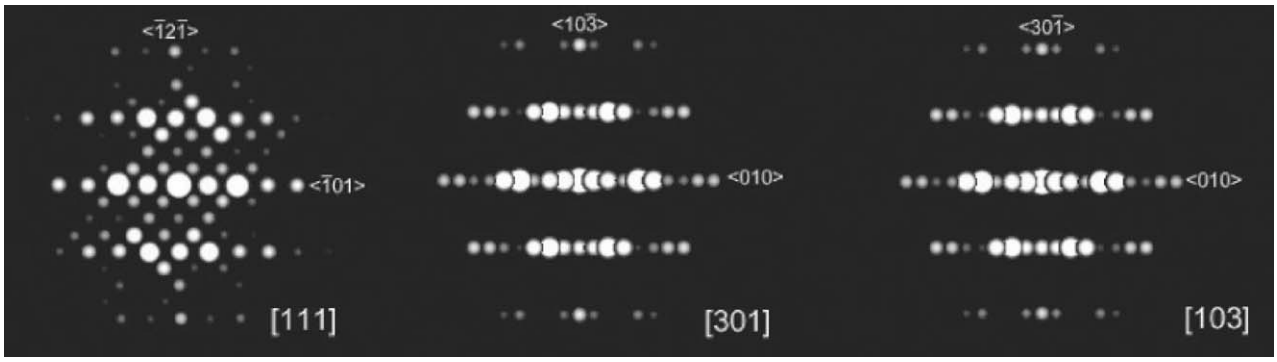

Fig. 7. Simulated ED patterns of a brownmillerite type structure viewed along [111], [301] and [103].

corresponding FFT. Computed simulated images are inserted in the right part of the image for clarity, using the coordinates for the brownmillerite type compound $Sr_2Co_{1.3}Ga_{0.7}O_5$ [13]. Fig. 3c shows an ED pattern recorded when tilting the crystallite in Fig. 3a around $\langle 010 \rangle_{per}$ (vertical in the image) 45° away from the zone-axis $\langle 001 \rangle_{per}$. In this pattern the reflections of the perovskite zone-axis pattern $\langle 101 \rangle_{per}$ can be clearly seen. After performing this 45° tilting around $\langle 010 \rangle_{per}$ from the superimposed $[101]_{BM}$ and $[010]_{BM}$ zone-axis patterns present in Fig. 3a, a superimposition of the brownmillerite zone-axis patterns $[100]_{BM}$, $[001]_{BM}$ and $[212]_{BM}$ should be found. This superimposition cannot be confirmed from Fig. 3c, since the $[212]_{BM}$ zone axis ED pattern has only the subcell reflections of perovskite and the [001] reflections at positions were the $[100]_{BM}$ should also have reflections. For clarity this is shown in Fig. 5 by means of simulated ED patterns of the $[100]_{BM}$, $[001]_{BM}$ and $[212]_{BM}$ zone axes. However, the FFTs of a corresponding HRTEM image confirm that the crystallites consist of intergrown brownmillerite domains. This is seen in Fig. 6 where FFTs of the domains *a*, *b* and *c* in the HRTEM image are presented, corresponding to the ED zone-axis patterns $[001]_{BM}$, $[100]_{BM}$ and $[212]_{BM}$, respectively. As mentioned above, no other reflections than those expected of a perovskite $\langle 101 \rangle_{per}$ ED zone axis pattern are present in the ED $[212]_{BM}$ zone-axis pattern. To confirm the zone axis orientation $[212]_{BM}$, the crystal can be tilted 18° around $\langle 010 \rangle_{per} = [10{-}1]_{BM}$ axis to the $[111]_{BM} = \langle 102 \rangle_{per}$ zone-axis, which in the case of a brownmillerite type domain exhibiting supercell reflections in addition to the perovskite reciprocal lattice. The resulting ED pattern can be seen in Fig. 3b, which is tilted 18° from Fig. 3c. The supercell reflections of the zone-axis pattern $[111]_{BM}$ can be clearly seen, along with reflections from the overlapping $[103]_{BM}$ and $[301]_{BM}$ zone-axis patterns, as expected when tilting 18° from the $[001]_{BM}$ and $[100]_{BM}$ zone axes, respectively. Simulated zone-axis patterns $[111]_{BM}$, $[103]_{BM}$ and $[301]_{BM}$ are shown in Fig. 7.

4. Discussion

From the ED patterns and the HRTEM images it can be concluded that the perovskite super-structure of $Sr_2Co_{2-x}Al_xO_5$, $x = 0.3 - 0.5$, is of brownmillerite type. The crystallites consist of intergrown domains of an *I*-centred brownmillerite. *I*-centring could be concluded since the reflection condition $hkl : h + k + l = 2n$ was found when indexing the ED pattern with the brownmillerite type unit cell. The perovskite subcell parameters are very close to each other, and therefore peak splitting could not be seen in the XRD. The small size of the domains may be an explanation of the peculiarities of the XRD patterns for $Sr_2Co_{2-x}Al_xO_5$ $x = 0.3 - 0.5$.

The situation in $Sr_2Co_{2-x}Al_xO_5$ $(0.3 \leqslant x \leqslant 0.5)$ very much resembles that reported for $SrFe_{1-x}V_xO_{2.5+x}$ $(0.05 \leqslant x \leqslant 0.1)$ [16], where an XRD investigation revealed the presence of the cubic perovskite structure, but a transmission electron microscopy investigation showed the crystallites to consist of small domains, about 2×10^5 Å^3 in size, having brownmillerite type structure. The authors suggested V^{5+} and O^{2-} to be enriched at domain boundaries, indicating the ordered regions to consist mostly of $Sr_2Fe_2O_5$ with brownmillerite structure. This suggested the domain structure to be caused by the presence of additional oxygen in the structure. Similar domain structure has also been reported in the system $Ca_2Fe_xMn_{2-x}O_{6-\gamma}$ [17]. In the case of $Sr_2Co_{2-x}Al_xO_5$ iodometric titration gave no indications of additional oxygen atoms. Moreover, it is not likely that cobalt in an oxidation state higher than 3+ should be stable at the high synthesis temperatures used for the present compound. One might assume the domain structure of the prepared compounds to be caused by inhomogeneous distribution of cobalt and aluminium in the crystallites. In this case domain boundaries should be enriched in cobalt or aluminium. The reason for this would be the low reactivity of Al_2O_3 used for synthesis of $Sr_2Co_{2-x}Al_xO_5$ and, hence the necessity of using a higher temperature (1250°C) than for $Sr_2Co_{2-x}Ga_xO_5$,

which is synthesized at 1100°C and has a much more ordered structure [13].

Acknowledgments

The authors want to thank the Swedish Research Council and the Royal Swedish Academy of Sciences (KVA) for financial support. This work was partially supported by RFBR (03-02-32990). Acknowledgement is made to the donors of the American Chemical Society Petroleum Research Fund for support of this research (PRF ACS 38459-AC5). S.Ya.I. is indebted to the Scientific Council of MSU, and E.V.A. to the Russian Science Support Fund.

References

[1] A.M. Abakumov, M.G. Rozova, B.Ph. Pavlyuk, M.V. Lobanov, E.V. Antipov, O.I. Lebedev, G. van Tendeloo, O.L. Ignatchik, E.A. Ovtchenkov, Yu.A. Koksharov, A.N. Vasilév, J. Sol. Stat. Chem. 160 (2001) 353.
[2] A.J. Wright, H.M. Palmer, P.A. Anderson, C. Greaves, J. Mater. Chem. 12 (2002) 978.
[3] A.M. Abakumov, M.G. Rozova, B.Ph. Pavlyuk, M.V. Lobanov, E.V. Antipov, O.I. Lebedev, G. van Tendeloo, D.V. Sheptyakov, A.M. Balgurov, F. Bourée, J. Sol. Stat. Chem. 158 (2001) 100.
[4] A. Colville, S. Geller, Acta Cryst. B 27 (1971) 2311.
[5] A. Colville, S. Geller, Acta Cryst. B 28 (1972) 3196.
[6] R. Arpe, R. von Schenk, H. Mueller-Buschbaum, Z. Anorg. Allg. Chem. 410 (1974) 97.
[7] C. Greaves, A.J. Jacobsen, B.C. Tofield, B.E.F. Fende, Acta Cryst. B 31 (1975) 641.
[8] P. Berastegui, S.-G. Eriksson, S. Hull, Mat. Res. Bull. 34 (1999) 303.
[9] O.H. Hansteen, H. Fjellvåg, B.C. Hauback, J. Sol. Stat. Chem. 141 (1998) 411.
[10] T. Takeda, Y. Yamaguchi, H. Watanabe, J. Phys. Soc. Jpn. 33 (1972) 970.
[11] S. Lambert, H. Leligny, D. Grebille, D. Pelliquin, B. Raveau, Chem. Mater. 14 (2002) 1818.
[12] J.T. Vaughey, J.B. Wiley, K. Poeppelmeier, Z. Anorg. Allg. Chem. 598 (1991) 327.
[13] F. Lindberg, S.Ya. Istomin, P. Berastegui, G. Svensson, S.M. Kazakov, E.V. Antipov, J. Sol. State Chem. 173 (2003) 395.
[14] R. Kilaas, 2000, http://ncem.lbl.gov/.
[15] P.D. Battle, T.C. Gibb, A.T. Steel, J. Chem. Soc. Dalton Tran. 10 (1987) 2359.
[16] N. Nakayama, M. Takano, S. Inamura, N. Nakanishi, K. Kosuge, J. Solid State Chem. 71 (1987) 403.
[17] J.M. González-Calbet, M. Vallet-Regí, J. Alonso, J. Rodríguez-Carvajal, J. Fontcuberta, J. Solid State Chem. 81 (1989) 1.